Macromolecules

ARTICLE

pubs.acs.org/Macromolecules

Systematic Dielectric Relaxation Study of Solid-Like Polyelectrolyte−Surfactant Complexes formed between Poly(styrenesulfonate) and Cationic Surfactants

Kenji Nakamura* and Koji Fukao

Department of Physical Sciences, Ritsumeikan University, Kusatsu, Shiga 525-8577, Japan

ABSTRACT: The dielectric relaxation behavior of polyelectrolyte−surfactant complexes with ordered lamellar microstructure were studied using broadband dielectric spectroscopy technique in the frequency range of 0.1 Hz to 2 MHz. We employed four complex samples formed between poly(styrenesulfonate) and didodecyldimethylammonium or alkyltrimethylammonium with various alkyl chain length. Three dielectric relaxation modes were observed in all complexes. The fastest and slowest relaxation modes showed Arrhenius temperature dependence. The fastest relaxation mode is attributed to motions of a surfactant grafted onto a polymer chain, whereas the slowest relaxation mode is attributed to the motions of an ion-pair formed between a negatively charged electrolyte monomer unit in a polymer and positively charged headgroup in a surfactant molecule. The intermediate relaxation mode showed Vogel−Fulcher−Tamman temperature dependence, and accordingly it derived from the segmental motion of the polymers forming intralamellar loops, interlamellar bridges or cilia. The slowest relaxation mode strongly correlates to the conductivity of the system, which indicates that surfactant ions are transported by the repetition process of formation and dissociation of ion-pairs.

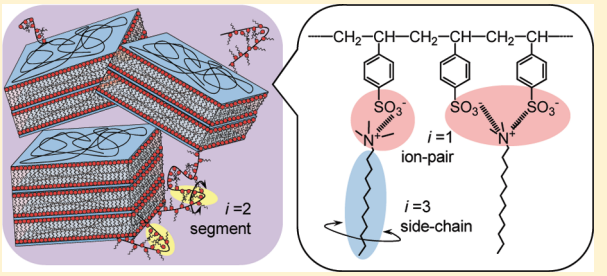

INTRODUCTION

Polyelectrolytes form many kinds of molecular assemblies with surfactants due to intermolecular electrostatic and hydrophobic interactions in aqueous solution.[1−4] A mixture of fully charged polyelectrolytes and oppositely charged surfactants in aqueous solution, especially, yields water-insoluble polyelectrolyte−surfactant complexes (PSCs) due to the stoichiometric, strong 1:1 electrostatic interaction caused between a surfactant molecule and a monomer unit of the polyelectrolytes.[3−8] PSCs are dissolved into organic solvents and produce films via film casting technique similar to ordinary polymers.

Antonietti and his co-workers have first investigated the structure of the PSCs of poly(alkyltrimethylammonium styrenesulfonate) series using small and wide-angle X-ray scattering (SAXS and WAXS) measurements.[9] These PSCs were formed by a polyion, poly(styrenesulfonate), and cationic surfactants, alkyltrimethylammonium with different alkyl chain lengths. These PSCs showed a highly ordered lamellar microstructure with a long period of ca. 2.9−4.0 nm. Antonietti also reported the PSCs with ordered structure of a cylindrical morphology[10] or helical conformation.[11] Since materials with highly ordered structure are often utilized for functionalized membranes or films, PSCs have received much research attention for their potential application.[5,8,12−14]

In terms of thermodynamics or mechanics, PSCs are classified into two types, i.e. solid-like and liquid-like.[15] Solid-like PSCs exhibit a glass transition above the thermal decomposition temperature; consequently they are unable to be molded to produce plane films with a hot press technique. On the other hand, glass transition temperature (T_g) of liquid-like PSCs is observed at temperatures below their thermal decomposition temperature. Liquid-like PSCs become rubbery with increasing temperature as in the case of the ordinary elastomers.[16]

Dielectric relaxation (DR) measurements are powerful tools to investigate the motions of molecules over a broad time range, on the order of 10^{-11} to 10^{2} s.[17,18] DR behavior of PSCs were investigated by Antonietti in 1990s.[15,16] They investigated the DR behavior of both liquid-like and solid-like PSCs and found that these PSCs exhibited a β-relaxation mode. This was attributed to the motion of the surfactant chains grafted into the polyelectrolytes because the β-relaxation mode showed Arrhenius temperature dependence irrespective of the PSC species. The liquid-like PSC system consisting of poly(diallyldimethylammonium) and soybean lecithin showed not only the β-relaxation mode but also the second relaxation mode around 190 K.[16] Conductivity of solid-like PSCs showed Arrhenius temperature dependence, in contrast, that of liquid-like PSCs showed Vogel−Fulcher−Tamman (VFT) temperature dependence.

Despite the pioneering works studied by Antonietti and coworkers, DR measurements of PSCs were mainly performed at lower temperatures (> room temperature) due to the high conductivity of PSCs. If the effect of direct current conductivity is strong, it often masks DR modes within DR spectra and

Received: December 9, 2010
Revised: March 9, 2011
Published: March 30, 2011

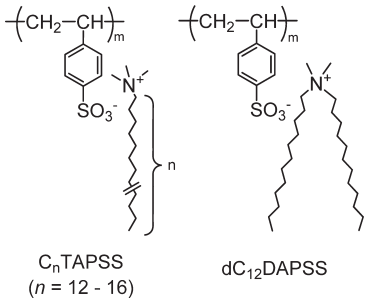

Figure 1. Chemical structure of poly(alkyltrimethylammonium styrenesulfonate) (C_nTAPSS) with various alkyl chain length n and poly(didodecyldimethylammonium styrenesulfonate) (dC_{12}DAPSS).

hinders the deconvolution of the DR spectra into each relaxation mode. Recently, Wübbenhorst proposed a novel method to eliminate the contribution of direct current conductivity from the DR spectra.[21] With the use of this analysis, DR studies of ionomers[19,20] were successful in proving the presence of novel DR mode due to the motion of ion-pairs formed between electrically charged monomer units on a polymer chain and oppositely charged counterions. Since PSCs are specified into one of the polyelectrolytes, they would show the relaxation modes due to ion-pairs and others.

In this study, we reinvestigated the DR behavior of the PSCs over a wide frequency range from 0.1 Hz to 2 MHz and wide temperature range from −90 to 180 °C. In order to clarify the micro dynamics of PSCs, we chose the PSC series of poly(alkyltrimethylammonium styrenesulfonate) (C_nTAPSS) with various alkyl chain length, n, and poly(didodecyldimethylammonium styrenesulfonate) (dC_{12}DAPSS) (Figure 1). According to Antonietti et al., C_nTAPSS are classified into solid-like PSCs, which form the ordered lamellar microstructure.[9,15] Antonietti et al. have investigated the DR behavior of C_{14}TAPSS and observed the β-relaxation mode at the temperature range of −15 to −110 °C.[15] Our systematic DR studies of C_nTAPSS and dC_{12}DAPSS proved the presence of novel relaxation modes including the ion-pair mode.

EXPERIMENTAL SECTION

Materials. Polystyrene ($M_n = 4.0 \times 10^5$, $M_w/M_n = 1.09$) was used as a precursor to poly(sodium styrenesulfonate) NaPSS, which was purchased from Polymer Source Inc. (Montreal). Cationic surfactants, dodecyltrimethylammonium bromide (C_{12}TAB), tetradecyltrimethylammonium bromide (C_{14}TAB), cetyltrimethylammonium bromide (C_{16}TAB) and didodecyldimethylammonium bromide (dC_{12}TAB), were purchased from Wako Pure Chemicals (Osaka, Japan). Deuterated chloroform ($CDCl_3$) and deuterated water (D_2O) were purchased from ISOTEC Inc. (Cambridge, U.K.) and used as a solvent for NMR measurements. All of the reagents were used without further purification. Highly deionized water with a specific resistance of >16 MΩ cm, obtained using Elix system (Japan Millipore, Tokyo, Japan), was used as the pure water.

Synthesis. NaPSS was synthesized from polystyrene via the fully sulfonation technique using H_2SO_4 and P_2O_5 proposed by Vink.[22] The degree of sulfonation of the polymer sample was determined by the neutralizing titration method with aqueous NaOH solution and estimated to be 94%. The neutralized NaPSS was dialyzed against water (pH = 9) for more than 4 days and obtained as a powder via freeze-drying. The purity of NaPSS was confirmed using ^{1}H NMR measurement in D_2O.

Table 1. Density, ρ, and Long Period, l_{lam}, of the Lamellar Microstructure Order for C_nTAPSS and dC_{12}DAPSS, and Length or Width, l_s, of a Tetragonal Monomer unit in the Lamella Phase with l_s Equal to the Hopping Length, λ, of Surfactant Ions

	ρ/g cm^{-3}	l_{lam}/nm	$l_s(\cong\lambda)$/nm
C_{16}TAPSS	1.08	3.56	0.636
C_{14}TAPSS	1.05	3.24	0.655
C_{12}TAPSS	1.08	3.10	0.639
dC_{12}DAPSS	0.980	2.86	0.819

C_nTAPSS and dC_{12}DAPSS were prepared by mixing NaPSS and a slight excess of cationic surfactants, C_nTAB and dC_{12}DAB, respectively, in an aqueous solution at room temperature. Resultant precipitates were washed with water until the rinsed solution remained clear with the addition of an aqueous $AgNO_3$ solution. After the excess salt and surfactant were eliminated from the products, C_nTAPSS or dC_{12}DAPSS were dried under vacuum at 60 °C. The purity of C_nTAPSS or dC_{12}DAPSS was confirmed using ^{1}H NMR measurement in $CDCl_3$.

Measurements. ^{1}H NMR measurements were performed using a NMR spectrometer (JNM-ECA-400, JEOL, Tokyo, Japan) with a proton resonance frequency of 400 MHz to characterize the synthesized NaPSS and PSCs at 30 °C.

Small and wide-angle X-ray scattering (SAXS and WAXS) measurements were performed on the BL40B2 beamline at SPring-8. The wavelengths of X-rays were 0.9 and 0.7 Å for SAXS and WAXS measurements, respectively. The detector used in our measurements was a combination of X-ray image intensifier and CCD camera. The positional resolution of the CCD camera was 0.106 mm in both the horizontal and vertical directions. The camera lengths were 2099 and 517 mm for SAXS and WAXS measurements, respectively. The obtained scattering data were corrected in order to remove variations in intensities of incident X-rays and the contribution of background scattering.

Dielectric relaxation measurements were performed using two measuring systems. The LCR meter (E4980A, Agilent, CA) was used for an angular frequency (ω) range of 1.36×10^2 to 1.36×10^7 rad s^{-1}. The impedance analyzer, (SI1260, Solartron Instruments, Hampshire, U.K.) including the dielectric measurement interface (SI1296, Solartron Instruments, Hampshire, U.K.), was used for ω ranging from 6.28×10^{-1} to 6.28×10^6 rad s^{-1}. The obtained real and imaginary part of electric capacitance (C' and C'') were converted to the real and imaginary part of the relative electric permittivity (ε' and ε'') using the relationships $\varepsilon' = C'C_0^{-1}$ and $\varepsilon'' = C''C_0^{-1}$, with a vacant capacitance (C_0).

Density, ρ, of C_nTAPSS and dC_{12}DAPSS were determined using picnometer with decane as filled solvent at 25 °C. Obtained ρ values are summarized in Table 1.

The sample film for density, dielectric relaxation and X-ray measurement was prepared as follows. C_nTAPSS/$CHCl_3$ or dC_{12}DAPSS/$CHCl_3$ solution was cast onto a Teflon Petri dish. After slow evaporation of the solvent, the plane films were dried under vacuum at 70 °C. The resulting C_nTAPSS and dC_{12}DAPSS films seemed translucent. The film thickness of PSCs were 39 μm for C_{16}TAPSS, 47 μm for C_{14}TAPSS, 88 μm for C_{12}TAPSS, and 84 μm for dC_{12}DAPSS, respectively. For DR measurement, Au was vacuum deposited onto both faces of the films to serve as electrodes. The sample films were then mounted inside the homemade sample cell, in which the temperature was controlled by the combination of a heater (DSSP23, Shimaden, Tokyo, Japan) and a chiller (UT-2000, EYELA, Tokyo, Japan). Since C_nTAPSS and dC_{12}DAPSS possess hygroscopic properties, they were dried under vacuum at 60 °C for 4 h and were heated at 180 °C for 20 min under normal pressure before the DR measurements. The measurement temperatures ranged from −90 to +180 °C.

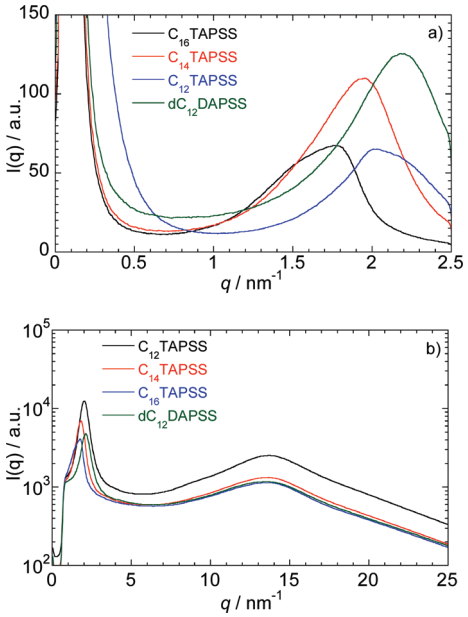

Figure 2. (a) SAXS and (b) WAXS diffractograms for C_nTAPSS and dC_{12}DAPSS films at 25 °C.

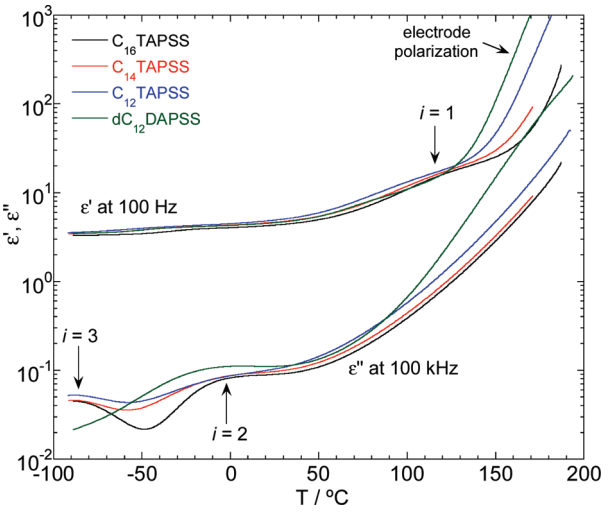

Figure 3. Dependence of real and imaginary parts of electric permittivities, ε' and ε'', at 100 Hz and 100 kHz, respectively, on temperature T for C_nTAPSS and dC_{12}DAPSS.

RESULTS

Microstructure of C_nTAPSS and dC_{12}DAPSS. Antonietti investigated microstructure of C_nTAPSS with n = 12, 14, 16, and 18 using SAXS and WAXS measurements and found that the C_nTAPSS series formed lamellar microstructures.[9] We also confirmed the microstructure of not only C_nTAPSS but also dC_{12}DAPSS using SAXS and WAXS measurements (Figure 2, parts a and b, respectively). The SAXS and WAXS diffractograms for C_nTAPSS and dC_{12}DAPSS show the scattering peak at the scattering vector, q, range of 1.8−2.2 nm^{-1} and a broad amorphous peak around q = 13.6 nm^{-1}.

The former scattering peaks have been also observed in the Antonietti study.[9] We simply estimated the long periods, l_{lam}, for our PSCs from the q value of the maximum peak. Obtained l_{lam} values are tabulated in Table 1. These values of long period for C_nTAPSS are slightly higher than those estimated by Antonietti.[9] The facts that obtained l_{lam} increases with increasing n values of C_nTAPSS and approximately equals to the twice the alkyl chain length of surfactants (all trans configuration) suggests these PSCs form lamellar microstructure like lipid bilayers.[23] It is important to note that higher order peaks due to lamellar microstructure were not observed in our PSCs. The long-range order peaks has been also absent for the same system studied by Antonietti.[9] Hence, C_nTAPSS and dC_{12}DAPSS are unlikely to form the multilamellar structures.

One may think SAXS diffractograms for C_{16}TAPSS and C_{12}TAPSS exhibit double peaks. In the lamellar phase, alkyl tail of a certain surfactant interpenetrates into the alkyl tail of the surfactant at the opposite side of lamellas.[9] Long period of lamellas should be not monodisperse but widely ranged because of the various interpenetration extent of surfactants in lamellas. This would cause the SAXS curve broadness and the double peak.

Dielectric Relaxation Behavior of C_nTAPSS. Figure 3 shows the temperature dependences of ε' at 100 Hz and ε'' at 100 kHz for the C_nTAPSS series. Remarkably sharp increases in ε' and ε'' curves were observed in the higher temperature regime at over 120 and 50 °C, respectively. This increase in the ε' and ε'' curves is due to the electrode polarization behavior and the direct current conductivity of the sample, respectively. Three DR modes were observed in the C_nTAPSS system, irrespective of the alkyl chain length n of the incorporated surfactants. The first relaxation mode (i = 1) was found in the ε' spectrum at around 100 °C. The second (i = 2) and third (i = 3) relaxation modes were observed in the ε'' curve at around 0 and −90 °C, respectively. Since these relaxation temperatures seem to be independent of the C_nTAPSS species, the origin of the each relaxation mode for C_nTAPSS was considered to be the same. We chose the C_{16}TAPSS system as a typical example for C_nTAPSS species and discuss its precise DR behavior.

Figure 4a shows the DR spectra, ε' and ε'', on the angular frequency, ω, for C_{16}TAPSS at various temperatures. The sharp increases in the ε' and ε'' curves in the lower frequency regime at temperatures over 110 °C is due to the electrode polarization effect and the direct current conductivity of the sample, respectively. This frequency dispersion profile also provides the three DR modes as in the case with the temperature dispersion profile (Figure 3). Clear DR due to the i = 3 mode was observed in the frequency regime $\omega > 10^4$ rad s^{-1} at −90 °C. The ε'' spectrum at −30 °C reveals a rather broad relaxation due to the i = 2 mode in the frequency regime $10^2 < \omega < 10^6$ rad s^{-1}. The DR mode i = 1 was observed in terms of the ε' spectrum at temperatures over 110 °C. The effect of direct current conductivity was so strong that it masked the i = 1 mode in the ε'' spectrum.

In order to subtract the contribution of the direct current conductivity from ε'' spectrum, we employed the following equation.

$$\varepsilon''_{der} = -\frac{\pi}{2}\frac{\partial\varepsilon'(\omega)}{\partial(\ln\omega)} \quad (1)$$

This equation provides an approximately conduction-free ε'' spectrum in the frequency regime where ε' contains no electrode polarization effects.[21,24] We also evaluated another conduction-free ε'', $\Delta\varepsilon''$, to confirm the validity of ε''_{der} using the following

dx.doi.org/10.1021/ma102808y |Macromolecules 2011, 44, 3053–3061

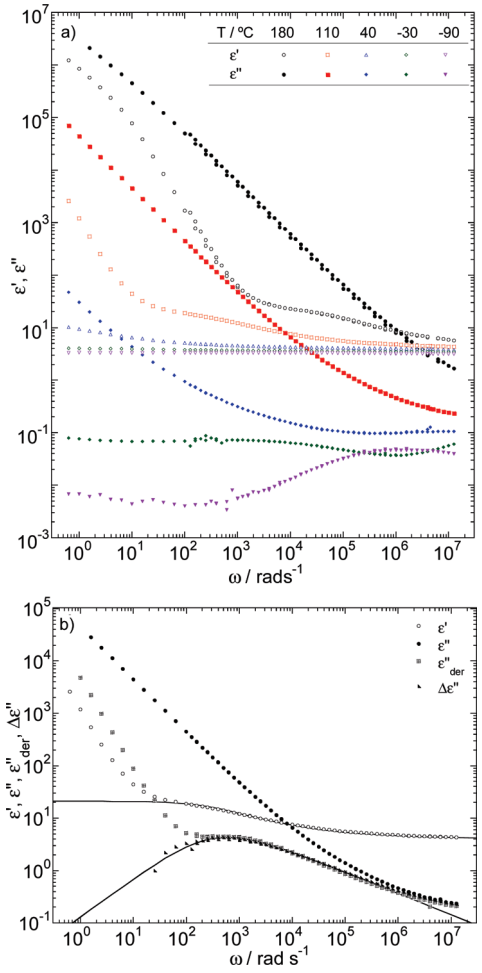

Figure 4. (a) Dependence of ε' and ε'' on angular frequency, ω, for C_{16}TAPSS at various temperatures. (b) Dependence of ε', ε'', imaginary part of the electric permittivities following elimination of the contributions of direct current conductivity, ε''_{der} and $\Delta\varepsilon''$, calculated using eqs 1 and 2, respectively, on ω for C_{16}TAPSS at 110 °C. Solid lines represent the best fit curves for ε' and ε''_{der} ($\Delta\varepsilon''$) calculated using eq 3.

equation.

$$\Delta\varepsilon'' = \varepsilon'' - \frac{\kappa}{\omega\varepsilon_0} \qquad (2)$$

where ε_0 is the permittivity of a vacuum and κ is the specific direct current conductivity evaluated from the plateau value of $\kappa(\omega) = C''\omega\varepsilon_0 C_0^{-1}$. This equation simply subtracts the contribution of the direct current conductivity from the ε'' spectrum. Figure 4b shows the dependence of ε', ε'', ε''_{der}, and $\Delta\varepsilon''$ on ω for C_{16}TAPSS at 110 °C. The correspondence between ε''_{der} and $\Delta\varepsilon''$ supports the validity of regarding ε''_{der} (or $\Delta\varepsilon''$) as the conduction-free ε'' spectra. ε''_{der} and $\Delta\varepsilon''$ curves reveal the maximum peak at the frequency where the ε' spectra show the DR mode $i = 1$.

Since the relaxation mode due to the electrode polarization effect is not an essential relaxation mode reflecting the motions of polymers and surfactants incorporated in PSCs, we took the DR modes $i = 1-3$ into account and ignored the electrode polarization relaxation mode in the curve fitting procedure of the DR spectra. We used ε''_{der} spectra as the loss spectra instead of ε'' spectra for the fitting procedure. DR spectra of C_{16}TAPSS were

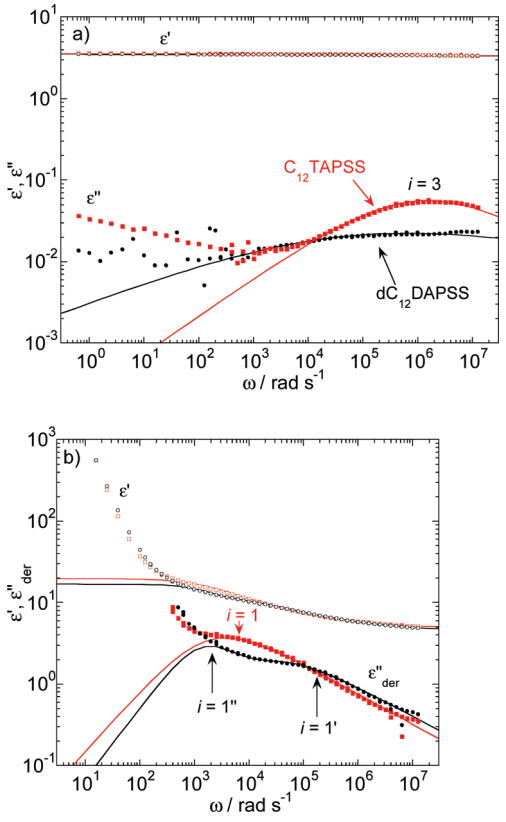

Figure 5. Angular frequency ω dependence of (a) ε' and ε'' for C_{12}TAPSS and dC_{12}DAPSS at −90 °C and (b) ε' and ε''_{der} for C_{12}TAPSS and dC_{12}DAPSS at 120 °C. Solid lines indicate the best fit curves for ε' and ε'' (ε''_{der}) calculated using eq 3. In order to describe the DR spectrum for dC_{12}DAPSS at 120 °C, two relaxation modes, $i = 1'$ and $1''$, are necessary.

well described as the summation of three Havriliak−Negami type relaxation formulas, which corresponds to the DR modes $i = 1-3$, as follows.

$$\varepsilon^* = \sum_{i=1}^{3} \frac{\varepsilon_i}{(1 + (i\omega\tau_i)^{p_i})^{q_i}} + \varepsilon_\infty \qquad (3)$$

Here ε_i and τ_i represent dielectric relaxation strength and time for the relaxation mode i, respectively, and p_i, q_i are the broadening factors of the relaxation mode i. We employed nonlinear least-squares approach with minimizing the reduced variance for fitting DR spectra with eq 3. Figure 4b includes a typical example of the best fit curves for ε' and ε''_{der} (or $\Delta\varepsilon''$) calculated using eq 3 with parameters of $\varepsilon_\infty = 4.1$, $\varepsilon_1 = 17.0$, $\tau_1 = 3.5 \times 10^{-3}$ s, $p_1 = 0.75$, $q_1 = 0.55$ for C_{16}TAPSS at 110 °C. Since the $i = 2$ and 3 modes are out of the frequency range at 110 °C, ε_∞ includes the contribution of both ε_2 and ε_3. Other DR spectra for the C_nTAPSS system at any given temperature were also described by eq 3 with broadening parameters $p_1 = 0.72-0.75$, $q_1 = 0.50-0.75$, $p_2 = 0.28-0.35$, $q_2 = 1$, $p_3 = 0.46-0.65$, and $q_3 = 0.90$.

These results deviate from the DR studies by Antonietti and his co-workers.[15] They investigated DR behavior of C_{14}TAPSS at temperatures ranging from −15 to −110 °C and found that only the β-relaxation mode derived from the motions of surfactants incorporated in PSCs were observed. In their measurement temperature range, DR mode $i = 1$ is the out of the frequency range. However DR mode $i = 2$ and 3 were clearly observed in the

dx.doi.org/10.1021/ma102808y |*Macromolecules* 2011, 44, 3053–3061

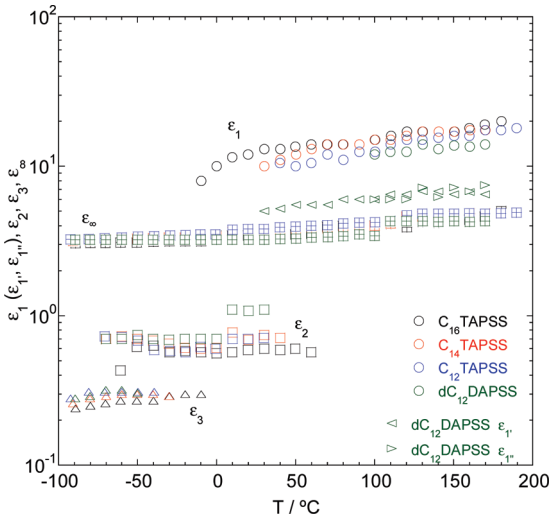

Figure 6. Dependence of the relaxation strength, ε_1 ($\varepsilon_{1'}$ and $\varepsilon_{1''}$), ε_2 and ε_3, for each relaxation mode and high frequency limiting permittivity, ε_∞, on T for C_nTAPSS and dC_{12}DAPSS. The values of ε_∞ at high temperatures include the contributions of ε_3 or both ε_3 and ε_2 because the $i = 2$ and 3 modes were out of the measurement frequency regime at high temperatures.

temperature range from −10 to −90 °C (Figure 4a). We suspect that their β-relaxation mode would include both the $i = 2$ and 3 modes that are found in our study. Since the DR spectra of C_{14}TAPSS obtained by Antonietti seems noisy in the frequency regime over 10 kHz at low temperatures, they were unable to discern the lower temperature relaxation mode (DR mode $i = 3$ in our study) from the observed one (DR mode $i = 2$ in our study).

Dielectric Relaxation Behavior of dC_{12}DAPSS. Figure 3 shows the dependence of ε' at 100 Hz and ε'' at 100 kHz on temperature T for dC_{12}DAPSS. dC_{12}DAPSS exhibited the DR mode $i = 1$ and 2 as in the case for C_nTAPSS series, but seems to lack the DR mode $i = 3$ around the temperature of −90 °C. Figure 5a focuses on the DR spectrum for dC_{12}DAPSS at −90 °C. For comparison, Figure 5a includes the DR spectrum for C_{12}TAPSS at −90 °C. One can confirm the presence of the DR mode $i = 3$ in the ε'' spectrum for dC_{12}DAPSS. However, DR mode $i = 3$ for dC_{12}DAPSS has a rather broad relaxation time distribution than that for C_{12}TAPSS. This DR mode for dC_{12}DAPSS can be described by eq 3 (black solid line) with parameters of $\varepsilon_\infty = 3.22$, $\varepsilon_3 = 0.28$, $\tau_3 = 2.0 \times 10^{-5}$ s, $p_3 = 0.26$ and $q_3 = 0.50$ as in the case with C_{12}TAPSS (red solid line) with parameters of $\varepsilon_\infty = 3.24$, $\varepsilon_3 = 0.30$, $\tau_3 = 8.0 \times 10^{-7}$ s, $p_3 = 0.47$ and $q_3 = 0.90$.

DR mode $i = 1$ for dC_{12}DAPSS is also different from that for C_nTAPSS system. Figure 5b shows the dependence of ε' and ε''_{der} on ω for dC_{12}DAPSS and C_{12}TAPSS at 120 °C. As shown in the red solid line, DR mode $i = 1$ for C_{12}TAPSS is well described by the sum of a unique Havriliak−Negami formula and ε_∞ with parameters of $\varepsilon_\infty = 4.70$, $\varepsilon_1 = 15.0$, $\tau_1 = 6.0 \times 10^{-4}$ s, $p_1 = 0.90$ and $q_1 = 1.00$. However, the DR spectra for dC_{12}DAPSS were unable to be described by a single relaxation formula but are well reproduced by a sum of two Havriliak−Negami formulas labeled $i = 1'$ (higher frequency one) and $1''$ (lower frequency one) modes. The black solid lines in Figure 5b are the best fit curves for the DR spectra of dC_{12}DAPSS using a sum of two Havriliak−Negami formulas and ε_∞ with parameters of $\varepsilon_\infty = 4.30$,

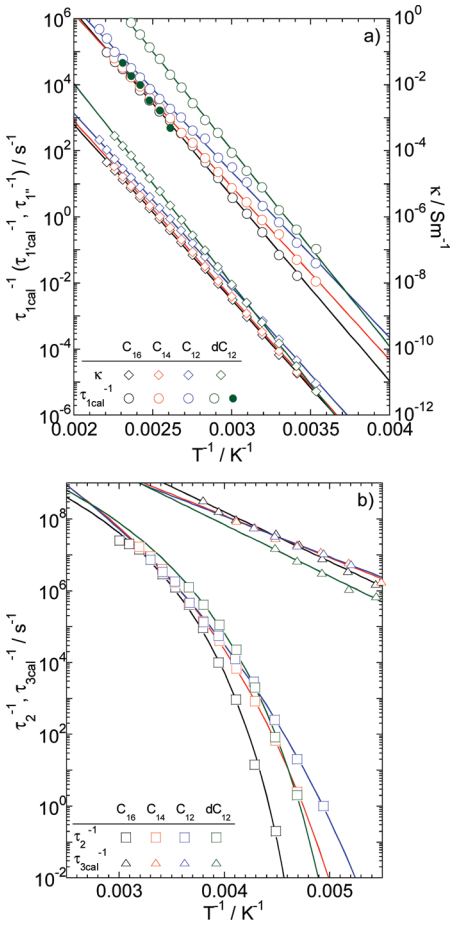

Figure 7. Arrhenius plot of (a) reciprocal of $\tau_{1\ cal}$ ($\tau_{1'cal}$; open symbol and $\tau_{1''cal}$; closed symbol) and specific direct current conductivity, κ, for C_nTAPSS and dC_{12}DAPSS and (b) reciprocal of τ_2 and $\tau_{3\ cal}$ for C_nTAPSS and dC_{12}DAPSS.

$\varepsilon_{1'} = 6.50$, $\tau_{1'} = 4.0 \times 10^{-5}$ s, $p_{1'} = 0.75$, $q_{1'} = 0.48$, $\varepsilon_{1''} = 6.00$, $\tau_{1''} = 6.0 \times 10^{-4}$ s, $p_{1''} = 0.90$ and $q_{1''} = 1.00$.

The origin of the DR modes $i = 1$−3 observed in C_nTAPSS series should be identical to those observed in dC_{12}DAPSS because these PSCs consist of a pair of the same polyelectrolyte and slightly different cationic surfactant molecules, possessing either a single or double long alkyl chains. The significant differences between dC_{12}DAPSS and C_nTAPSS found in DR mode $i = 1$ and 3 imply that the origin of these DR modes may involve motions of surfactants in the PSC.

Relaxation Strength and Times. Figure 6 shows the temperature dependence of the relaxation strength ε_1 (includes $\varepsilon_{1'}$ and $\varepsilon_{1''}$ for dC_{12}DAPSS), ε_2, ε_3 and ε_∞ for the C_nTAPSS and dC_{12}DAPSS obtained from the fitting procedure. ε_1 ($\varepsilon_{1'}$ and $\varepsilon_{1''}$) for all PSCs slightly increased with increasing temperature, but ε_2 and ε_3 for all PSCs remained constant. The values of $\varepsilon_{1'}$ and $\varepsilon_{1''}$ for dC_{12}DAPSS are similar to each other and the sum of $\varepsilon_{1'}$ and $\varepsilon_{1''}$ (shown as a green circle) is similar to ε_1 values for C_nTAPSS. This result suggests that the origin of the relaxation mode $i = 1'$ and $1''$ for dC_{12}DAPSS is the same as that of the relaxation mode $i = 1$ for the C_nTAPSS system. However, our DR study was unable to explain why the DR mode $i = 1$ is divided into two modes, $i = 1'$ and $1''$ mode, in the dC_{12}DAPSS system. Since DR mode $i = 2$ and 3 shifted to a higher frequency regime, with

dx.doi.org/10.1021/ma102808y |*Macromolecules* 2011, 44, 3053–3061

Table 2. Activation Energy, E, of τ_{1cal} ($\tau_{1'cal}$), τ_3 and Specific Direct Current Conductivity, κ, and Vogel Temperature, T_0, of τ_2 for C_nTAPSS and dC_{12}DAPSS[a]

	E/kJ mol^{-1}			T_0/K
	$\tau_{1\ cal}$	$\tau_{3\ cal}$	κ	τ_2
C_{16}TAPSS	111	27	102	180
C_{14}TAPSS	101	23	102	138
C_{12}TAPSS	95	22	101	113
dC_{12}DAPSS	111[a]	36	116	162

[a] These values are obtained from the Arrhenius plot profiles (Figure 7a and 7b) calculated using eqs 5 and 6.

increasing temperature, and ultimately moved out of the measurement frequency range, ε_∞ includes the contribution of ε_3 or both ε_3 and ε_2 at high temperatures. Though ε_∞ seems to slightly increase with increasing temperature in Figure 6, ε_∞ is virtually constant with respect to temperatures without these contributions.

If one employs the asymmetrical Cole−Davidson or Havriliak−Negami fitting equation to describe a DR spectrum, the obtained relaxation time does not reflect the frequency maximum in the loss spectrum. We used the following conversion to obtain the calibrated relaxation time, τ_{ical}, which corresponds to the reciprocal of the frequency at the peak of the ε''_{der} spectrum for DR mode i.[17]

$$\tau_{ical}^{-1} = \tau_i^{-1}\left(\sin\frac{p_i\pi}{2+2q_i}\right)^{1/p_i}\left(\sin\frac{p_iq_i\pi}{2+2q_i}\right)^{-1/p_i} \quad (4)$$

If the asymmetric broadening factor q_i is unity, τ_{ical} corresponds to τ_i. Since q_2 for C_nTAPSS series and $q_{1''}$ for dC_{12}DAPSS system are unity, we use τ_2 for C_nTAPSS and $\tau_{1''}$ for dC_{12}DAPSS as they are without the calibration of eq 4. Figure 7 summarizes the temperature dependence of (a) $\tau_{1\ cal}$ ($\tau_{1'cal}$ and $\tau_{1''}$), κ and (b) τ_2, $\tau_{3\ cal}$ for C_nTAPSS and dC_{12}DAPSS as an Arrhenius plot profile. κ curves for C_nTAPSS and dC_{12}DAPSS seem to coincide with each other except that for dC_{12}DAPSS system at higher temperatures. $\tau_{3\ cal}$ values at a given temperature are independent of the C_nTAPSS species. Whereas, $\tau_{3\ cal}$ for dC_{12}DAPSS is shorter than those for C_nTAPSS. At a given temperature, the values of $\tau_{1\ cal}$ for C_nTAPSS are similar to the values of $\tau_{1''}$ (green closed circle) for dC_{12}DAPSS but longer than $\tau_{1'cal}$ (green open circle) values for dC_{12}DAPSS. κ, $\tau_{1\ cal}$ ($\tau_{1'cal}$) and $\tau_{3\ cal}$ for C_nTAPSS and dC_{12}DAPSS show an Arrhenius temperature dependence (solid lines) represented as:

$$\tau_{1cal}^{-1} \quad \text{or} \quad \tau_{3cal}^{-1} \quad \text{or} \quad \kappa \propto \exp\left(-\frac{E}{RT}\right) \quad (5)$$

where R is the gas constant and E is the activation energy. The values of E for κ, $\tau_{1\ cal}$ ($\tau_{1'cal}$) and $\tau_{3\ cal}$ for C_nTAPSS and dC_{12}DAPSS are summarized in Table 2. On the other hand, τ_2 for both C_nTAPSS and dC_{12}DAPSS system shows the VFT temperature dependence as

$$\tau_2^{-1} \propto \exp\left(\frac{U}{T-T_0}\right) \quad (6)$$

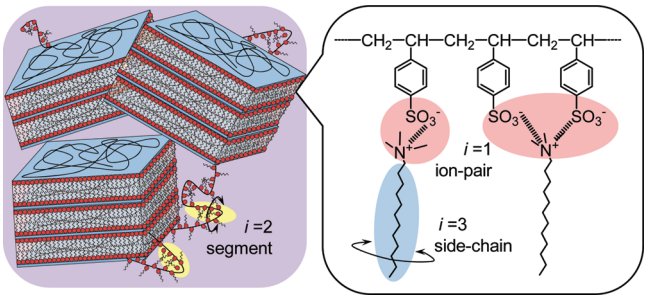

Figure 8. Schematic representation of the origin of the dielectric relaxation modes i = 1−3.

where U is the activation temperature and T_0 is the Vogel temperature at which the molecular dynamics reflecting the relaxation mode i = 2 should stop. Table 2 also includes T_0 values of $\tau_{2\ cal}$ for C_nTAPSS and dC_{12}DAPSS.

DISCUSSION

Mechanism of the Relaxation Mode i = 1 and Conductive Behavior. The values of E for $\tau_{1\ cal}$ ($\tau_{1'cal}$) and κ seem to be independent of the PSC species used in our study (Table 2). The values of E for $\tau_{1\ cal}$ ($\tau_{1'cal}$) (95−111 kJ mol^{-1}) approximately correspond with those of κ (101−116 kJ mol^{-1}). This finding indicates that the origin of the DR mode i = 1 correlates with the ion conduction of the PSCs. In ionomer systems, it has been shown that conductivity correlates to the DR mode regarding segmental motion of polymers, and both the segmental DR time and conductivity of ionomers show VFT temperature dependence.[19,20,25,26] Thus, the DR mode i = 1 of our PSCs, whose time constant shows Arrhenius temperature dependence as in the case for their conductivity, cannot be assigned to the segmental relaxation mode of polymers in PSCs.

We assign the DR mode i = 1 to the formation and dissociation process of ion-pairs formed between a negatively charged styrenesulfonate monomer (SS^-) unit in a poly(styrenesulfonate) (PSS^-) chain and a positively charged headgroup in a surfactant molecule (Figure 8). Ion-pair DR modes are known to be observed in systems such as ionomers,[19,20] aqueous polyelectrolyte solutions,[27] and aqueous surfactant solutions.[28,29] In these systems, ion condensation between a cation and an anion occurs. Since PSC consists of a pair of polyelectrolytes and surfactants, it seems natural that PSC exhibits the DR mode due to ion-pair motions.

If ion-pairs possess low kT, quadrupoles can be expected to form through dipole−dipole interactions of neighboring ion-pairs.[19] Since quadrupoles have no dipole moment, they do not contribute to an increase in dielectric strength. Quadrupoles should dissociate into two ion-pairs with increasing temperature, which results in an increment to the dielectric strength regarding ion-pair mode. Therefore, the finding that ε_1 slightly increases with increasing temperature (Figure 6) strongly supports the attribution of the DR mode i = 1 as the ion-pair motion.

The cooperativity between conductivity and ion-pair motions (DR mode i = 1) found in our PSCs can be explained by assuming that the conductive agent of surfactants are transported through the repetition of the ion-pair formation and dissociation process between plural SS^- units like a baton of a relay race.[30] We estimated the hopping length, λ, of surfactants between plural SS^- units with assuming that C_nTAPSS or dC_{12}DAPSS monomer

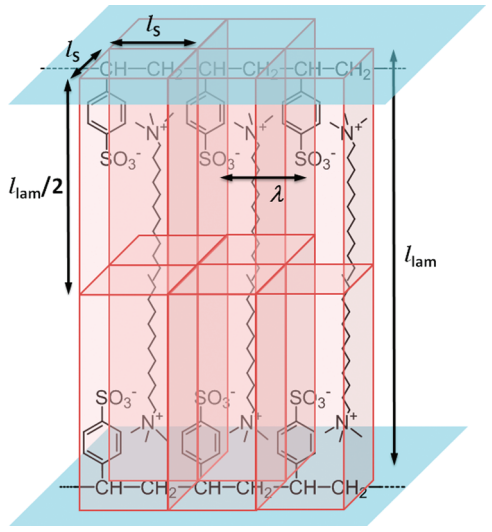

Figure 9. Schematic depiction of C_nTAPSS or dC_{12}DAPSS monomer units forming lamellar microstructure with the long period of l_{lam}. These monomer units are described as a red tetragonal structure with the height of $l_{lam}/2$ and width and length of l_s. λ means the hopping length of surfactants between plural SS^- units and equals to l_s.

unit in the lamella phase as tetragonal structure with the height of $l_{lam}/2$ and the length and width of l_s (Figure 9). The volume of C_nTAPSS or dC_{12}DAPSS monomer unit, v_m, provides the relationship $v_m = l_s^2 l_{lam}/2 = M/(\rho N_a)$, where M is the molecular weight of the monomer unit of PSCs and N_a is Avogadro's number, which allows us to evaluate the l_s values. The values of λ are obtained if ones permit the approximation of $l_s \cong \lambda$. Evaluated l_s (or λ) values are tabulated in Table 1. The values of l_s for C_nTAPSS are similar to each other but shorter than that for dC_{12}DAPSS. This finding is reasonable because the structure of a monomer unit of dC_{12}DAPSS is bulky in comparison with that for C_nTAPSS species. Obtained λ values are shorter than the segmental length of ordinary polymer (ca. 2.1 nm for bulk polystyrene[31]). Thus, a surfactant forming an ion-pair with a certain SS^- unit can easily change its interaction partner to another SS^- unit near the surfactant, and consequently the ion transport mechanism is controlled by the ion-pair motions rather than the segmental motions of polymers.

Mechanism of the i = 2 Relaxation Mode and T_0. DR mode i = 2 exhibits VFT temperature dependence, which indicates the molecular motion derived from the i = 2 mode should stop at a temperature of T_0. In general, DR modes due to segmental motion of ordinary polymers exhibit the VFT temperature dependence and strongly correlates to glass transition behavior.[17,18] The segmental motion becomes slow with decreasing temperature and finally stops around a temperature of $T_g - 50$ K. As mentioned above, C_nTAPSS and dC_{12}DAPSS are classified into the solid-like PSC, whose T_g is higher than the degradation temperature. This is confirmed by the experimental fact that our PSCs were unable to be molded to make plane films using the hot press technique. Hence, one supposes why the i = 2 mode exhibits VFT temperature dependence and what T_0 means.

We propose a hypothesis to explain the DR mode i = 2 and T_0 as follows. Some polymers near the edges of lamellas are not fully incorporated into lamellar phase but form intralamellar loops, interlamellar bridges or cilia (Figure 8) as observed in associative polymers in aqueous solution.[32] The 6% of the styrene monomer units in a PSS^- polymer enhance the desorption from lamellas because they would not have surfactant counterions. In the lamellar phase, motions of the polymers such as segmental motion are significantly restricted. On the other hand, motions of unassociated polymers forming loops, bridges or cilia are less restricted. The segmental motion of unassociated polymers becomes active and exhibits DR. The segmental motion of the unassociated polymers is attributed to the DR mode i = 2 and freezes at a temperature of T_0 (Figure 8). In other words, T_0 reflects the T_g of the unassociated polymers of PSCs.

This assumption is supported by the finding that T_0 increases with increasing n values of C_nTAPSS (Table 2) because hydrophobic interactions among surfactants grafted into PSS^- are enhanced by lengthening the alkyl chain in the surfactants. However differential scanning calorimetry measurements for C_nTAPSS and dC_{12}DAPSS at temperatures ranging from −150 to +200 °C did not show any thermal transitions clearly; further studies are necessary to understand the DR mode i = 2.

One may speculate that C_nTAPSS and dC_{12}DAPSS consists of both a lamellar and an amorphous phases like ordinary crystalline polymers,[33,34] and less restricted polymers in the amorphous phase shows the segmental DR mode at temperatures higher than T_0. However, our experimental and sample preparation temperatures are higher than T_0, polymers in the amorphous phase are able to diffuse and are immediately incorporated into growing lamellar phase, whose T_g is higher than experimental or degradation temperatures. This conclusion contradicts to the speculation of presence of both phases.

Mechanism of the Relaxation Mode i = 3. At a given temperature, $\tau_{3\ cal}$ values for the C_nTAPSS species are similar to each other, but shorter than those of dC_{12}DAPSS (Figure 7b). Moreover, ε'' curve corresponding to the i = 3 mode for dC_{12}DAPSS is broader than that of C_nTAPSS (Figure 5a). These findings indicate that the DR mode i = 3 is attributed to the motions of the surfactant alkyl chain grafted into the PSS^- chain (Figure 8) because motions of twin tail surfactants should be more restricted than the single tail surfactants.[35]

This attribution agrees with that of the β-relaxation mode observed in the C_{14}TAPSS studied by Antonietti and coworkers.[15] Relaxation times of their β-relaxation mode exhibited an Arrhenius temperature dependence as in the case for those of our DR mode i = 3. Moreover, the activation energy of their β-relaxation mode (36 kJ mol^{-1}) is similar to those of our DR mode i = 3 (22−36 kJ mol^{-1}). As mentioned in the Results, however, we found DR modes i = 2 and 3 in the measurement temperature regime studied by Antonietti (−15 to +110 °C).[15] Thus, the correspondences between our DR mode i = 3 and their β-relaxation mode regarding the temperature dependence behavior does not exactly support the validity of our attribution.

Degree of Dissociation of Surfactants. Degree of dissociation, f_{dis}, of surfactants from polymers were determined using the combination of Nernst−Einstein and Einstein−Smoluchowski equations.[36,37] These equations give

$$\kappa = \frac{n_{ion} q^2 \lambda^2}{2kT\tau_h} \qquad (7)$$

where n_{ion} is the effective number density of ions, q is the elementary charge, k is the Boltzmann constant, λ and τ_h is the hopping length and time of ions. Since τ_{ical} reflects the lifetime of ion-pairs, we simply took the relationship $\tau_h = \tau_{1\ cal}$ into consideration for C_nTAPSS system. On the other hand, both $i = 1'$ and $1''$ modes for dC_{12}DAPSS reflect the ion-pair motion as

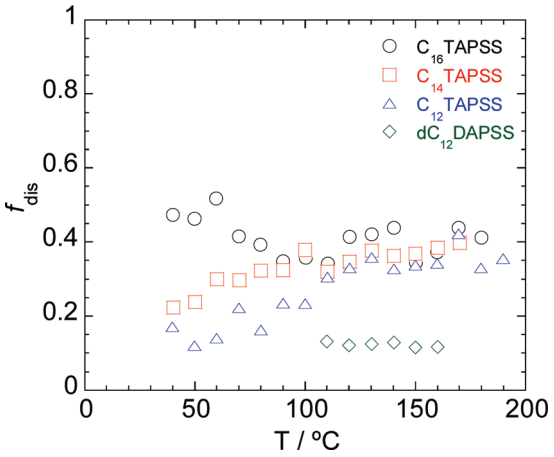

Figure 10. Relationship between degree of dissociation, f_{dis}, of surfactants from PSCs and T for C_nTAPSS or $dC_{12}DAPSS$.

discussed above, we calculated a harmonic average relaxation time, τ_{1har}, between $\tau_{1'cal}$ and $\tau_{1''}$ for $dC_{12}DAPSS$ as

$$\frac{1}{\tau_{1har}} = \frac{\varepsilon_{1'}}{\varepsilon_{1'} + \varepsilon_{1''}} \frac{1}{\tau_{1'cal}} + \frac{\varepsilon_{1''}}{\varepsilon_{1'} + \varepsilon_{1''}} \frac{1}{\tau_{1''}} \quad (8)$$

and regarded τ_{1har} as τ_h. Equation 8 is based on the assumption that the magnitude of the dipole moment due to $i = 1'$ ion-pair mode corresponds to that for $i = 1''$ ion-pair mode. These considerations and eq 7 lead us to obtain n_{ion} values. Then f_{dis} values are evaluated from the relationship $f_{dis} = n_{ion}M/(\rho N_a)$.

Figure 10 shows the relationship between f_{dis} values and T for the PSCs. At higher temperature regime, f_{dis} values for C_nTAPSS are similar to each other to show the value of ca. 0.40. On the other hand, f_{dis} values for $dC_{12}DAPSS$ (ca. 0.12) are lower than those for C_nTAPSS. This finding is reasonable because the hydrophobic interaction among twin tail surfactants, $dC_{12}DA^+$, is stronger than that among single tail surfactants, C_nTA^+. Note that the use of $\tau_{1'cal}$ or $\tau_{1''}$ instead of τ_{1har} leads us to obtain the f_{dis} values of ca. 0.06 or 2.1 (overestimated), respectively.

CONCLUSION

We investigated the dielectric relaxation behavior of polyelectrolyte−surfactant complexes consisting of poly(styrenesulfonate) and didodecyldimethylammonium ($dC_{12}DAPSS$) or alkyltrimethylammonium with various alkyl chain length n (C_nTAPSS). SAXS and WAXS measurements confirmed that $dC_{12}DAPSS$ and C_nTAPSS formed ordered lamellar microstructure. Both $dC_{12}DAPSS$ and C_nTAPSS showed the three dielectric relaxation modes. The fastest relaxation mode was assigned to motions of surfactant molecules grafted onto a polymer. Only the intermediate relaxation mode exhibited VFT temperature dependence. We assumed that certain polymers at the edge of lamellas form intralamellar loops, interlamellar bridges or cilia, and attributed the intermediate relaxation mode to the segmental motion of these unassociated polymers. The slowest relaxation mode and the conductivity exhibited Arrhenius temperature dependence with a similar activation energy, ca. 100 kJ mol^{-1}. This indicates that the slowest relaxation mode reflects the formation and dissociation process of ion-pairs and also denotes that the conductive agent of surfactants are transported through the repetition of the ion-pair formation and dissociation process between plural electrolyte monomer units (0.64−0.82 nm) in a polymer. Nernst−Einstein and Einstein−Smoluchowski analyses provided the degree of dissociated surfactants were 0.15−0.50 for C_nTAPSS and 0.12 for $dC_{12}DAPSS$.

AUTHOR INFORMATION

Corresponding Author

*E-mail: kenjin@se.ritsumei.ac.jp.

ACKNOWLEDGMENT

This work was supported by a Grant-in-Aid for Young Scientists (B) (No. 21750131) from the Japan Society for the promotion of Science. This work was also supported by the Sasakawa Scientific Research Grant from The Japan Science Society. The synchrotron radiation experiments were performed at the SPring-8 with the approval of the Japan Synchrotron Radiation Research Institute (JASRI).

REFERENCES

(1) Goddard, E. D. *Colloids Surf.* **1986**, *19*, 255.
(2) Goddard, E. D. *Colloids Surf.* **1986**, *19*, 301.
(3) Hayakawa, K.; Santerre, J. P.; Kwak, J. C. T. *Macromolecules* **1983**, *16*, 1642.
(4) Thünemann, A. F.; Müller, M.; Dautzenberg, H.; Joanny, J.; Löwen, H. *Adv. Polym. Sci.* **2004**, *166*, 113.
(5) Thünemann., A. F. *Prog. Polym. Sci.* **2002**, *27*, 1473.
(6) Ober, C. K.; Wegner, G. *Adv. Mater.* **1997**, *9*, 17.
(7) Kötz, J.; Kosmella, S.; Beitz, T. *Prog. Polym. Sci.* **2001**, *26*, 1199.
(8) Antonietti, M.; Faul., C. F. J. *Adv. Mater.* **2003**, *15*, 673.
(9) Antonietti, M.; Conrad, J.; Thünemann, A. *Macromolecules* **1994**, *27*, 6007.
(10) Antonietti, M.; Conrad, J. *Angew. Chem., Int. Ed.* **1994**, *33*, 1869.
(11) Wenzel, A.; Antonietti, M. *Adv. Mater.* **1997**, *9*, 487.
(12) Thünemann, A. F. *Adv. Mater.* **1999**, *11*, 127.
(13) Thünemann, A. F.; Beyermann, J. *Macromolecules* **2000**, *33*, 6878.
(14) Behnke, M.; Tieke, B. *Langmuir* **2002**, *18*, 3815.
(15) Antonietti, M.; Maskos, M.; Kremer, F.; Blum, G. *Acta Polym.* **1996**, *47*, 460.
(16) Antonietti, M.; Neese, M.; Blum, G.; Kremer, F. *Langmuir* **1996**, *12*, 4436.
(17) Kremer, F., Schohals, A., Eds. *Broadband Dielectric Spectroscopy*; Springer-Verlag: Berlin, 2002.
(18) Runt, J., Fitzgerald, J. J., Eds. *Dielectric Spectroscopy of Polymeric Materials: Fundamentals and Applications*; American Chemical Society: Washington, DC, 1997.
(19) Fragiadakis, D.; Dou, S.; Colby, R. H.; Runt, J. *Macromolecules* **2008**, *41*, 5723.
(20) Fragiadakis, D.; Dou, S.; Colby, R. H.; Runt *J. Chem. Phys.* **2009**, *130*, 064907.
(21) Wübbenhorst, M.; van Turnhout, J. *J. Non-Cryst. Solids* **2002**, *305*, 40.
(22) Vink, H. *Makromol. Chem.* **1981**, *182*, 279.
(23) Taguchi, K.; Yano, S.; Hiratani, K.; Minoura, N.; Okahata, Y. *Macromolecules* **1988**, *21*, 3336.
(24) Steeman, P. A. M.; van Turnhout, J. *Macromolecules* **1994**, *27*, 5421.
(25) Klein, R. J.; Zhang, S.; Dou, S.; Jones, B. H.; Colby, R. H.; Runt, J. *J. Chem. Phys.* **2006**, *124*, 144903.
(26) Kline, R. J.; Welna, D. T.; Weikel, A. L.; Allcock, H. R.; Runt, J. *Macromolecules* **2007**, *40*, 3990.
(27) Nakamura, K.; Shikata, T. *Macromolecules* **2006**, *39*, 1577.
(28) Shikata, T.; Imai, S. *Langmuir* **1998**, *14*, 6804.
(29) Fernandez, P.; Schrödle, S.; Buchner, R.; Kunz, W. *ChemPhysChem* **2003**, *4*, 1065.

(30) Nakamura, K.; Saiwaki, T.; Fukao., K. *Macromolecules* **2010**, *43*, 6092.
(31) Inoue, T.; Onogi, T.; Yao, M. L.; Osaki, K. *J. Polym. Sci., Part B* **1999**, *37*, 389.
(32) Winnik, M. A.; Yekta, A. *Curr. Opin. Colloid Interface Sci.* **1997**, *2*, 424.
(33) Mandelkern, L. *Crystallization of Polymers*; Cambridge University Press: Cambridge, U.K., 2002.
(34) Strobl, G. R. *The Physics of Polymers: Concepts for Understanding Their Structures and Behavior*, 3rd ed.; Springer: New York, 2007.
(35) Israelachvili, J. N., Ed. *Intermolecular and surface forces*, 2nd ed.; Academic Press: London, 1991.
(36) Atkins, P.; de Paula, J. *Physical Chemistry*, 8th Ed.; Oxford University Press: Oxford, U.K., 2006.
(37) Sangoro, J. R.; Serghei, A.; Naumov, S.; Galvosas, P.; Kärger, J.; Wespe, C.; Bordusa, F.; Kremer, F. *Phys. Rev. E* **2008**, *77*, 051202.